15th International Congress of the Geological Society of Greece
Athens, 22-24 May, 2019 | Harokopio University of Athens, Greece
Bulletin of the Geological Society of Greece, Sp. Pub. 7 Ext. Abs. GSG2019-250

Stochastic Simulation of Seismic Motion and Site-Effects Studies of Ambient Noise and Seismic Data: The Case of the Vrisa Settlement and the 2017 M=6.3 Lesvos Earthquake

N. Chatzis[1], Ch. Kkallas[1], C. Papazachos[1], M. Anthymidis[1], Em. Rovithis[2], Ch. Karakostas[2], Ch. Papaioannou[2]

(1) Department of Geophysics, School of Geology, Aristoteles University of Thessaloniki, Thessaloniki, Greece, chatniko@geo.auth.gr
(2) Institute Of Engineering Seismology & Earthquake Engineering, Elaionon 28, Pylaia, Thessaloniki, Greece

A strong earthquake with magnitude M6.3 struck on June 12, 2017 the island of Lesvos and the surrounding area, situated at the north-east part of the Aegean Sea. While the mainshock epicenter was estimated to be ~15 km off the southern coast of Lesvos island with a focal depth to 12 Km, relatively limited damage was reported along the coastal Lesvos area. An exception was the historical settlement of Vrisa, where extensive damage (including a large number of collapsed masonry houses) was observed, mainly in the northwestern part of the village, which was located on recent (Holocene) sediments. On the contrary, for the remaining part of the village, founded on stiffer Neogene deposits, limited damage was reported. Moreover, the earthquake affected mainly the historical, masonry buildings of the village, with a negligible impact on the (fewer) reinforced concrete modern constructions.

To explain the presence of such localized damage phenomena, we employ the stochastic finite-fault modelling approach of Motazedian and Atkinson (2005), as adapted by Boore (2009), for the simulation of Fourier Amplitude Spectra (FAS) of the 2017 Lesvos earthquake. To calibrate the necessary model parameters of the stochastic finite-fault method, we used waveform data from both acceleration and broadband-velocity sensor instruments within ~100km from the earthquake fault. To constrain the mainshock focal parameters, we have computed an updated 1-D velocity model for the study area following Kissling et al. (1994), and relocated the Lesvos 2017 aftershock sequence in order to determine the main geometrical features of the earthquake's fault. Preliminary relocations were performed with the HYPOINVERSE (Klein, 2002) program, and hypoDD (Waldhauser, 2001) relocations allowed to obtain an improved aftershock sequence distribution. From the relocation procedure we constrained the main fault dimensions, strike and dip, in good agreement with fault plane solutions published for this event, and used them in the stochastic simulation approach. Using the previous source information, as well as appropriate path and generic site-effect information for the Aegean area, we solved for the mainshock stress-parameter value, in an attempt to fit the FAS of the mainshock recorded waveforms. To estimate the stress parameter ($\Delta\sigma$), we adopted a trial-and-error approach and tested different stress-drop values, through comparison of simulated and observed acceleration Fourier spectra.

Since the previously described damage pattern for the Vrisa settlement is indicative for the presence of strong site-effect phenomena, we have employed a large number of surface geophysical measurements, recording mainly of surface waves from both active and passive sources, in order to study the shallow geophysical structure and examine the spatial distribution of the expected site effects on seismic motions for the Vrisa area.

To determine the 1-D shear-wave velocity structure, a circular Noise-Array was realized in the northern (Holocene) Vrisa area (with a radius of 10, 40 and 100 m for the inner, the middle and the outer circle radius, respectively). Moreover, 23 lines of MASW were realized with the use of 4.5 Hz vertical geophones. This dataset was complemented by the performance of nearly 70 single station ambient noise measurements, which were conducted with the use of broad-band seismometers (CMG-6TD or CMG-40T-60 sec with Reftek 130 digitizers). Horizontal-to-Vertical Spectral Ratio (HVSR, Nakamura, 1989) curves were calculated for all noise recording sites, while dispersion curves were determined with the use of the f-k method, both for the MASW and the Noise-Array data.

For the final 1-D shear-wave velocity model determination we employed a joint inversion of Rayleigh wave dispersion curve and Rayleigh ellipticity information. For this reason, Rayleigh wave ellipticity was extracted from the noise recordings using the approach of Hobiger et al. (2009). Ellipticity was jointly inverted with the reconstructed Rayleigh dispersion curves, in order to increase the Vs-model penetration depth, as well as to reduce the non-uniqueness of the model inversion. The joint inversion was performed with the use of a Monte-Carlo approach, namely the neighborhood algorithm, as adapted by Wathelet et al. (2008) and realized through the *Geopsy* software tools (http://www/geopsy.org).

The final Vs models (figure 1) show the presence of a very soft layer (Vs<300 m/sec, in most cases <200m/s for the uppermost 10-15m), with a typical thickness of ~20-25 m for the northwestern part of Vrisa, clearly corresponding to the Holocene formations of the study area. This layer is underlain by a stiffer layer (Vs>500 m/sec, locally >700-800m/sec), which outcrops in the Vrisa southeastern section, corresponding to the Neogene formations. The transition from Neogene to Holocene formations is rather abrupt, suggesting the presence of a NE-SW normal fault that creates the local basin, which is filled with Holocene formations. Preliminary 1D site response analysis in the frequency domain for the final geophysical model of the Vrisa area confirms the presence of strong amplification of seismic motions in the northwestern Vrisa area, in good agreement with the damage pattern of the June 12, 2017 M6.3 earthquake.

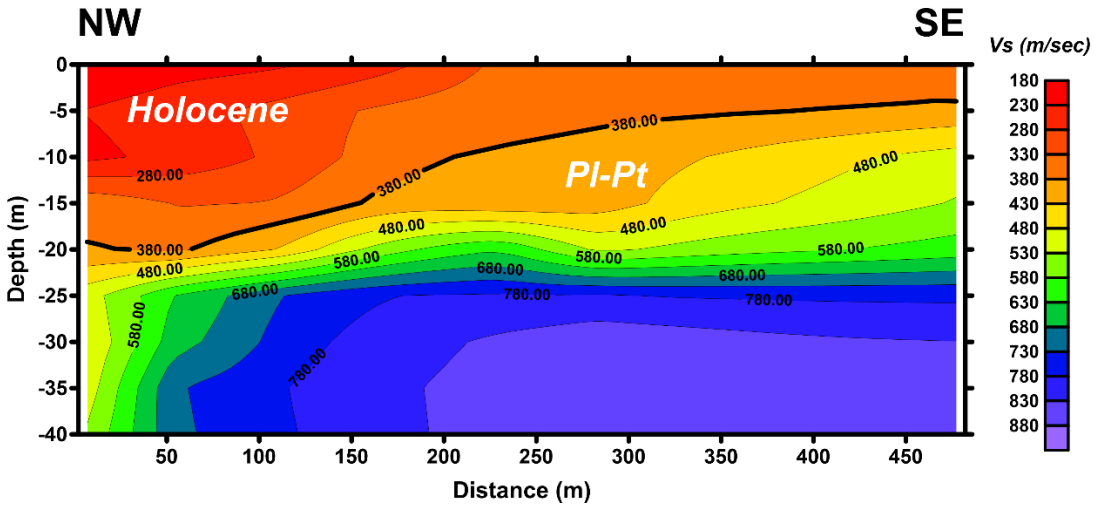

Figure 1. Final 2D model of shear-waves velocity along a NW-SE profile in the Vrisa area. The Holocene sediments with low S-wave velocities are located on the NW part of the study area, where the main damages and amplification of seismic motions from the strong earthquake at 12 June 2017 (M6.3) mainly occurred.

The HVSR results revel a strong spatial variation of the soil fundamental frequency, f_0, and maximum HVSR amplitudes, A_0^{HVSR}, with almost flat HVSR curves in the southeast Vrisa (Neogene sediments) and large A_0^{HVSR} values (locally larger than 5) in the Holocene sediments at frequencies f_0~2.5-3 Hz. Considering that A_0^{HVSR} values generally provide a low threshold of local amplifications, we expect seismic motions to be significantly amplified in the Holocene sediments section of the village. This was confirmed by computing Standard Spectral Ratios (SSR, Borcherdt, 1970) from aftershock records in both Neogene and Holocene deposits, which showed that peak amplifications, A_0, are almost double than the values provided by A_0^{HVSR}, though the resonant frequency, f_0, and spectral shapes of the SSR and HVSR curves were nearly identical. The spectral slopes (Anderson and Hough, 1984) were computed for all the sites with aftershock records, in order to compute kappa factors and the SSR curve correlations. By quantitative comparison of the HVSR and SSR results for several sites it was possible to determine an appropriate scaling factor and reduce all HVSR curves to equivalent SSR curves. Using these equivalent SSR amplifications, we employed the stochastic simulation method for the determination of complete ground motion simulations throughout a dense virtual receiver grid in the Vrisa area, and reconstructed the detailed spatial variation of several ground motion measures (PGA, PGV, etc.), as well as expected damages (IMM) in the broader Vrisa area. The results show that the while the southeastern part of the Settlement (Neogene deposits) exhibited values around IMM=6+ to 7, the northwestern Holocene section experienced damage levels of the order of IMM=8+ to 9, in excellent agreement with the observed damage distribution.

References

Anderson, J.G., Hough, S.E., 1984. A model for the shape of the Fourier amplitude spectrum of acceleration at high frequencies. Bulletin of the Seismological Society of America, 74(5), 1969-1993.

Boore, D.M., 2009. Comparing stochastic point-sou rce and finite-source ground-motion simulations: SMSIM and EXSIM. Bulletin of the Seismological Society of America, 99(6), 3202-3216.

Borcherdt, R.D., 1970. Effects of local geology on ground motion near San Francisco Bay. Bulletin of the Seismological Society of America, 60(1), 29-61.

Kissling, E., Ellsworth, W.L., Eberhart-Phillips, D., Kradolfer, U., 1994. Initial reference models in local earthquake tomography. Journal of Geophysical Research: Solid Earth, 99(B10), 19635-19646.

Klein, F.W., 2002. User's guide to HYPOINVERSE-2000, a Fortran program to solve for earthquake locations and magnitudes, USGS Open-File Report 2002-171, https://doi.org/10.3133/ofr02171

Hobiger M., Bard P-Y, Cornou C., Le Bihan N., 2009. Single station determination of Rayleigh wave ellipticity by using the random decrement technique (RayDec). Geophys. Res. Lett., 36, doi:10.1029/2009GL038863.

Motazedian, D., Atkinson, G.M., 2005. Stochastic finite-fault modeling based on a dynamic corner frequency. Bulletin of the Seismological Society of America, 95(3), 995-1010.

Nakamura, Y., 1989. A method for dynamic characteristics estimation of subsurface using microtremor on the ground surface. QR Railway Tech. Res. Inst., 30(1), 25-33.

Waldhauser, F., 2001. hypoDD--A program to compute double-difference hypocenter locations.

Wathelet, M., 2008. An improved neighborhood algorithm: Parameter conditions and dynamic scaling. Geophys. Res. Lett., 35, doi:10.1029/ 2008GL033256.